Capacity Investigations of MIMO Systems in Correlated Rician Fading Channel Using Statistical Clustered Modelling

Mohab A. Mangoud

Department of Electrical and Electronics Engineering
University of Bahrain, P.O.Box 32038, Isa Town, Kingdom of Bahrain
mangoud@eng.uob.bh

Abstract— In this paper the capacity of MIMO systems is investigated for different realistic propagation scenarios in Rician fading channel. A nonparametric stochastic model is presented and is used to develop the spatial fading correlation. Uplink statistical MIMO channel is assumed with Laplacian angular energy distributed over multi-clusters situations. Radio waves that are gathered in several clusters distributed over the space domain are assumed to exhibit different power profiles. Capacity investigations for both uniform linear array (ULA) and uniform circular array (UCA) for single cluster and multi-clustered assumptions are presented. The optimum selections of number of elements and spacing between elements are discussed for different values of Angle of Arrival (AoA) and Azimuth Spread (AS). Also, the impact of K factor of the Rician distribution for single and multi-clusters environments is studied under different propagation scenarios.

Index Terms— MIMO Systems, Statistical Channel Model, Capacity Investigations, Spatial Correlation, Power Azimuth Spectrum (PAS), Uniform Linear Array (ULA), Uniform Circular Array (UCA), Rician Fading.

I. INTRODUCTION

The spatial fading correlation of the channel has an adverse effect on the capacity of Multiple Input Multiple Output (MIMO) systems [1]. Accurately computing the spatial correlations is essential for predicting system performance. However, it is always a challenging task to evaluate the realistic correlation matrices with high accuracy due to the interdependence between the propagation environment and the antenna geometry and clustering of scatterers in the propagation environment. In [2]–[7],

stochastic none physical MIMO models with different assumptions about the scattering in the propagation environment and antenna geometries are considered. In these statistical clustered vector channel models, the groups of scatterers are modeled as clusters located around the antenna arrays. In [2] the parametric stochastic MIMO channel model is presented to estimate the performance of MIMO systems in terms of theoretical capacity. Cross-correlation functions of the received signal at two antenna elements with three different PAS (uniform, truncated Gaussian and truncated Laplacian). Exact expressions of the spatial correlation coefficients were derived for the different spatial distributions of AOD/AOA only for uniform linear arrays (ULAs). The model is applied for two case studies employing ULA array type, one for single cluster case and the other for bi-cluster assumption. For the antenna geometry selection, ULA is the most common geometry in cellular systems. However, UCA shows potential as an alternative geometry with its enhanced properties. Analysis of fading correlation was carried out for UCA in [3]–[5]. In the previous works the authors consider a single cluster model in Rayleigh channel. It is also known that the presence of LOS component along with the correlation between channel links may affect the capacity of the MIMO system [8]. In [8] analytical multivariable statistics is presented to obtain the upper bound for the pairwise error probability of the system under space time correlation Rician fast fading channel. However, the effect of Rician K factor on the capacity curves of correlated fading using simulation models need to be more investigated.

Thus, according to the previous discussion, the objective of this paper is to study the impact of having multi-clusters propagation scenarios and compares it with single cluster case for MIMO systems utilizing Hybrid ULA/UCA

configuration at both ends of Rician fading channel. This paper addresses the accuracy when modelling the spatially correlated MIMO channel using clustered channel model (that is developed from the models presented in [2]-[7]). The paper is organized as follows. In Section II, the nonparametric clustered MIMO model and special correlation matrix calculations are provided. In section III, the numerical results are presented for practical uplink MIMO system simulations with a detailed discussion for the numerical results. Some remarks will be carried out to highlight the effect of the choice of modelling assumptions on the capacity curves and the model applicability for practical systems. Finally, conclusions are derived in Section IV.

II. SPATIAL FADING CORRELATION AND CLUSTERED CHANNEL MODELS

Figure 1 shows a MIMO uplink scenario that is modeled in our investigations with transmitter at the mobile unite (MU) and receiver at the base station (BS). The channel is modeled as multi-clusters scattering environment which means that the signal will arrive at the BS from multiple Angles of Arrival (AoA) each with Azimuth spread (AS) that is a measure of the angle displacement due to the non-LOS propagation.
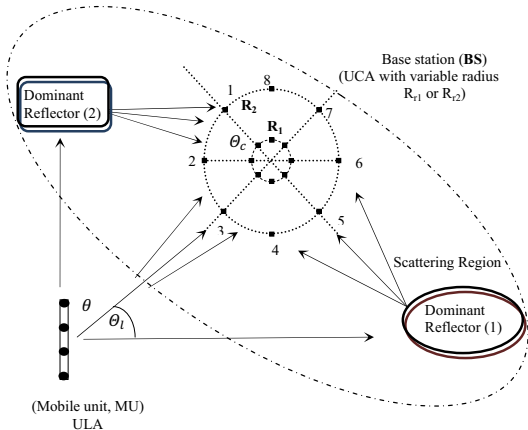

Fig. 1. Geometry of the MIMO system model of $M_t \times M_r$ elements ULA /UCA with signal arriving from multi-clusters in scattering channel.

As shown, (M_t) and (M_r) elements for transmit and receive arrays respectively are considered. The system is deploying ULA at MU, and a UCA or ULA at BS. The receive antenna UCA radius is assumed to be varied within the lower and upper bounds $\{R_1 : R_2\}$. Different number of elements M_r will be considered and uniformly spaced on either ULA/UCA configurations. Consider a signal arriving at the receive array from angle of arrival θ note that $\Theta_l = \frac{\pi}{2} - \Theta$. Thus, if a signal of interest can be described by the summation of signal arriving from angles with distribution $p_\Theta(\theta)$, then we know that the spatial correlation between two points a distance d apart can be determined as:

$$\rho(d) = \int_{-\pi}^{\pi} \left(e^{\frac{j2\pi d}{\lambda} \sin(\frac{\pi}{2} - \Theta)} \right) p_\Theta(\Theta) d\Theta \qquad (1)$$

For UCA this relation will be as follows

$$\rho(d) = \int_{-\pi}^{\pi} \left(e^{\frac{j2\pi R}{\lambda} \cos(\Theta - \phi)} \right) p_\Theta(\Theta) d\Theta \qquad (2)$$

where $p_\Theta(\theta)$ is considered here is any one of the distributions for multi-clustered Power Azimuth Spectrum (PAS), uniform, Gaussian and Laplacian [2], taking into account the unbalanced power in different clusters. In this paper, Laplacian distribution is considered where it is the best fit to measurement results in urban and rural areas. A multiclustered Laplacian PAS can be written as:

$$p_\Theta(\Theta) = \sum_{k=1}^{N_c} K_k e^{-a|\theta - \theta_{ok}|} \qquad (3)$$

where $(-\pi + \theta_{ok} \leq \theta \leq \theta_{ok} + \pi)$, θ_{ok} is the cluster k mean direction of arrival (AOA), N_c is the number of clusters. $K_k = \frac{a}{1 - e^{-a\pi}}$, is the normalization factor for each cluster to make $p_\Theta(\Theta)$ a density function and a is a decay factor which is related to the angle spread (AS). For ULA, the real and imaginary parts of the receiving spatial correlation between m[th] and n[th] elements using the integral in eq. (1) are given in [2] for the three PAS distributions. Also, in [4] it is shown that receiving correlation coefficients for UCA can be expressed by solving the integral in eq. (2) and by applying truncated Laplacian distributed as

$$Re\{R_{sr}(m, n)\} = J_o(Z_c) +$$
$$4K \sum_{k=1}^{\infty} \frac{a^2(1 - e^{-a\pi})}{a^2 + 4k^2} J_{2k}(Z_c) \cos[2k(\theta + \alpha)]$$
$$(4)$$

$$Im\{R_{sr}(m,n)\} =$$
$$4K \sum_{k=0}^{\infty} \frac{a(1-e^{-a\pi})}{a^2+(2k+1)^2} J_{2k+1}(Z_c) .$$
$$\sin\left[(2k+1)(\theta+\alpha)\right]$$
(5)

where Z_c is related to antenna spacing and α is the relative angle between the mth and n^{th} . For the ULA transmitting side, it is assumed that the mean angle of departure θ_t is uniformly distributed over $[0, 2\pi]$ that is given in [3] and it can be expressed as:

$$R_{st}(p,q) = J_o\left(2\pi \frac{(q-p)D_t}{\lambda}\right).$$
(6)

where D_t is the distance between elements p and q. The uplink spatial fading correlation $R_s(mp, nq)$ is the spatial correlation between the link from transmit antenna (p) to receive antenna (m) and the link from transmit antenna (q) to receive antenna (n). Defining $R_{st}(p,q)$ and $R_{sr}(m,n)$ as the spatial correlation due to the transmitter and receiver antennas respectively. Since the two links are statistically independent then the link spatial correlation can be divided into transmit part and receive part as

$$R_s(mp,nq) = R_{sr}(m,n) \times R_{st}(p,q).$$
(7)

The correlated Rician Fading MIMO channel Matrix, (T) with dimensions ($M_t \times M_r$) at one instance of time can be modelled as a fixed (constant, LOS) matrix and a Rayleigh (variable, NLOS) matrix.

$$T = \sqrt{\frac{K}{1+K}}\overline{H_{ric}} + \sqrt{\frac{K}{1+K}}R_r^{1/2}H_w R_t^{1/2} .$$
(8)

where H_w are zero mean and unit variance complex Gaussian random variables that presents the coefficients of the variable NLOS matrix. K is the Rician K-factor and R_r and R_t are the $M_r \times M_r$ and $M_t \times M_t$ correlation matrices that include all possible coefficients of spatial correlations between the channel links seen at transmit and receive elements respectively. Assuming equal power transmission across the array elements at the transmitter, the capacity of MIMO system can be computed from:

$$C = log_2\left[det\left(I_{Mr} + \frac{SNR}{Mt}TT^H\right)\right].$$
(9)

where T is the complex matrix given from (8), SNR is the average signal to noise ratio, and

I_{Mr} is the identity matrix with dimensions $M_r \times M_r$.

III. NUMERICAL RESULTS

In this section, the numerical analysis of spatial fading correlation and capacity investigations are presented for practical uplink application that is shown in Fig. 1. The impact of receiving antenna elements separation (in case of ULA) or circle radius (in case of UCA) on spatial correlations for single and two-clustered at different AoA and AS is illustrated in Figs. 2–5. Fig. 2 shows the spatial correlation $R_s(21,11)$ for 4 elements ULA receiver when the arriving signal is concentrated in single cluster, when the mean AoA, $\theta= 0$, 45 and 90 for two values of the variance of angular distributions, AS=2 and 20. As expected Rs decreases as D_r increases and as AS increases. The same is also observed for UCA in Fig. 3 where $R_s(21,11)$ is plotted versus the radius of 4 elements UCA. Comparing Figs. 2 and 3, it is seen that ULA experiences the lowest Rs at $\theta=90$ (broadside case, i.e the signal is arriving normal to array line) while the highest values is observed at the endfire case. However, for the UCA lower bound correlation curve is found to be at $\theta=45$, while the higher bound curves are observed at $\theta= 0$ and 90 having the same values. Figs. 4 and 5 show the $R_s(21,11)$ for 4 elements ULA and UCA receivers verse elements spacing and array circle radius respectively for 2 clusters case. Note that $R_s(21,11)$ and $R_s(31,41)$ are equal, since spacing and orientation between elements 1 and 2 are the same as 3 and 4. Here, AoA distribution is generated by two dominant reflectors, where signals impinge the antenna from two clusters that are assumed to be {[0, 0], [-45, 45], [-90, 90]}. R_s is computed by applying bi-modal PAS function for the laplacian distribution using eq. (3) considering N_c=2. As seen in Figs. 4 and 5 the correlation function has an oscillation term that depends on the difference between the AoA's of the two modes. As seen, the oscillation is slow for D_r versus ULA and for R versus UCA if the angles are close such as [-45, 45] case and the oscillation is faster when the two AoA's separation is large as the case of [-90, 90]. Comparing the envelope of the correlation
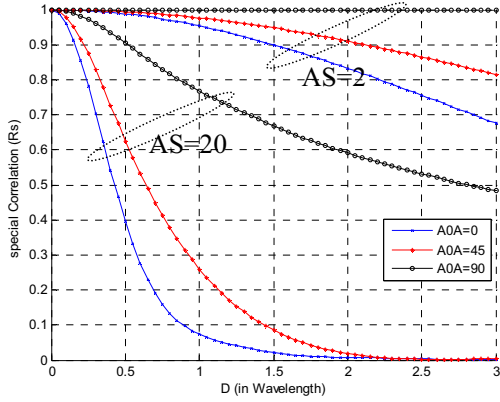
Fig. 2. Spatial correlation versus distance between elements for ULA configuration for laplacian distribution with 1 clusters have AS=20, AoA={0 45 90}.
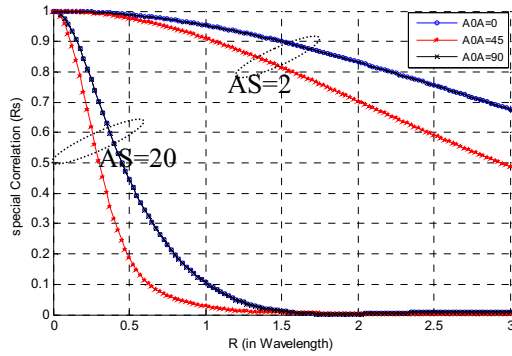

Fig. 3. Spatial correlation versus distance between elements for UCA configuration for laplacian distribution with 1 clusters have AS=2 & 20, AoA={0 45 90}.
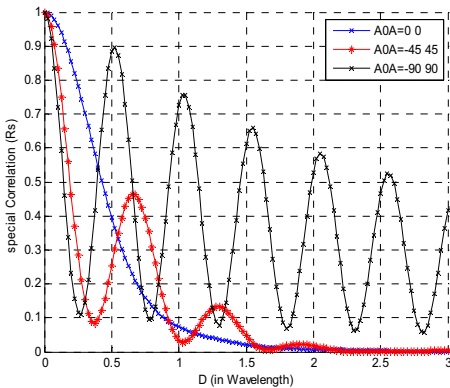

Fig. 4. Spatial correlation versus distance between elements for ULA configuration for laplacian distribution with 2 clusters have AS=20, AoA={[0 0],[-45 45],[-90 90]}.
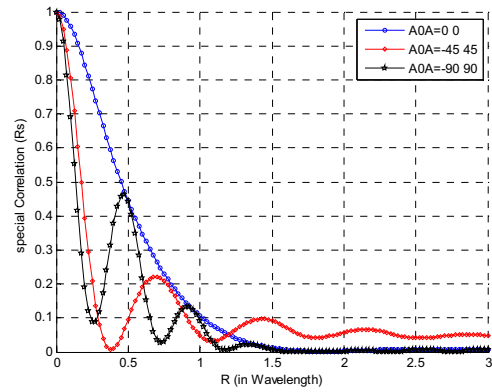

Fig. 5. Spatial correlation versus Radius of the array circle for elements(3,4) /(1,2) for UCA configuration for laplacian distribution with 2 clusters have AS=20, AoA={[0 0],[-45 45],[-90 90]}.
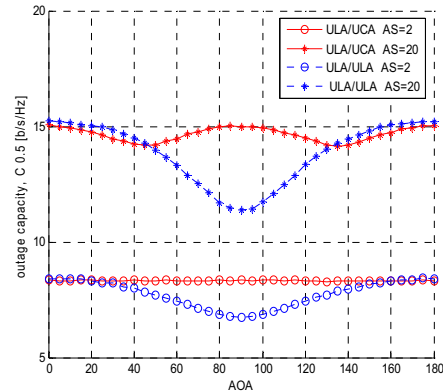

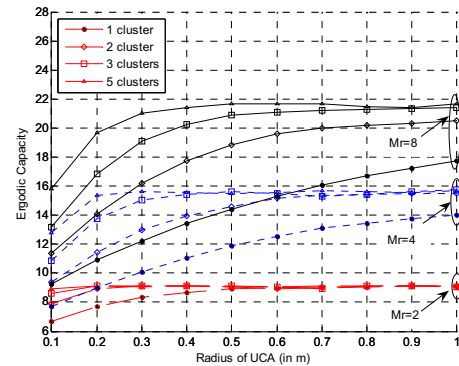Fig. 6. Ergodic Capacity versus AoA, one cluster case, 4x4 MIMO ULA and UCA system, SNR=15 dB.

Fig. 7. Ergodic capacity versus Radius (in wavelength) of UCA for 4x M_r MIMO system, where M_r =2, 4 and 8, As=10, SNR=15 dB.
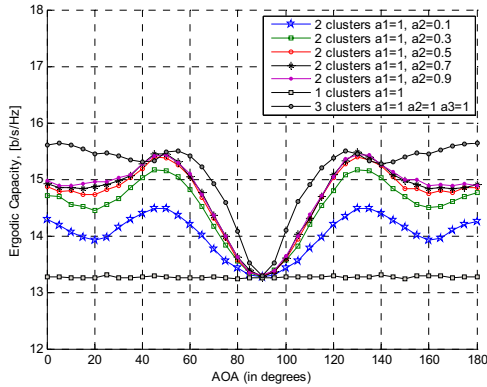
Fig. 8. Ergodic Capacity versus AoA, for 4x4 MIMO system UCA with AS=10 and SNR =15 dB. 1, 2 and 3 clusters, 1 cluster AoA=90, 2 clusters AoA={90, ϕ}, 3 clusters={0+ϕ, 90, 180-ϕ}.
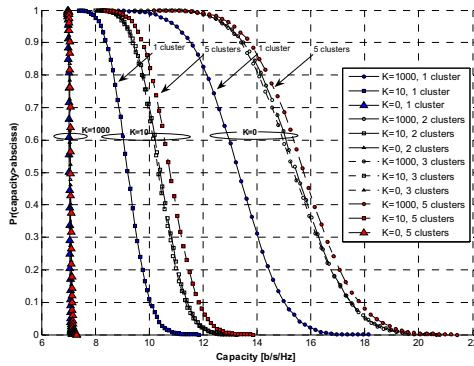

Fig. 9. Complementary CDF of the capacities of single and multi-clusters 4x4 MIMO cases, at different *K*-factor [0,10,1000] and SNR= 15dB, AS=10.
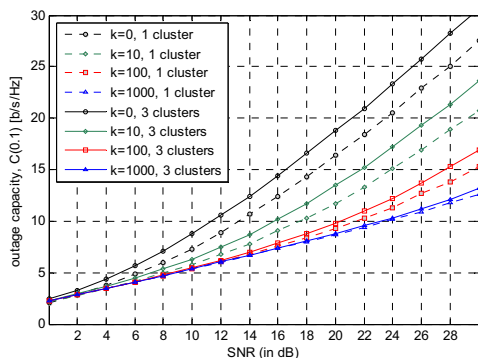

Fig. 10. Capacity vs. SNR for single and 3-clusters 4x4 MIMO cases, at different K-factor [0,10,1000], AS=10.

function for both configurations with two clusters in Figs. 4 and 5 it can be seen that the envelope correlation R_s has lower values for

UCA when compared to the ULA values. Next, Figs. 6–8 present capacity investigations for both ULA and UCA in single and multi-clustered for various number of elements, spacing between elements, AoA's and AS. Fig. 6 shows the ergodic capacity of the UCA and the ULA at the receiver as function of Θ_l and Θ_c (AoA). These results are performed for 4×4 MIMO system and for 10,000 channel realizations.

For a fair comparison between the two geometries, aperture size should be made the same (i.e. diameter of UCA = length of ULA). Thus, for ULA spacing D_r =0.5λ, the UCA radius is assumed to be R=0.75λ. Note that the elements are distributed evenly over both arrays. In this figure, capacity is investigated for AS = 2 (low) and AS=20 (high) while SNR is fixed at 15 dB for the two cases. As shown, the UCA outperforms the ULA in particular for small angle spread at endfire (Θ_l=90°). However, the ULA has nearly the same performance as UCA for certain angles-of-arrival (e.g., near broadside of the ULA $\Theta_l = 0°$ and 180°). It is also noted that the UCA has its lowest capacity at Θ_c=45° and 135° since in these two case two elements are directly behind and parallel to the other two elements (strongly correlated); this can be observed more at high AS.

Fig. 7 illustrates variations of ergodic capacity (at SNR=15 dB) versus variations of UCA radius in the range from {R_l=0.1λ} to {R_2=λ}. As shown in Fig. 1, this is performed for 4×M_r MIMO system, where M_r is assumed to be {2, 4 and 8} for different number of clusters {1, 2, 3 and 5} with mean AOA's {[90], [45, 90], [45, 90, 135], and [0, 45, 90, 135, 180]} respectively. All clusters are assumed to have AS=10. As can be seen in Fig. 6, capacity increases as radius of the UCA increases where the elements experience lower correlation. Also, higher capacity is observed when more clusters are included in the model. This effect increases as the number of elements increases, and this is clear when comparing curves for 2, 4 and 8 elements. It is also seen that for the 5 cluster model the capacity reaches its maximum and becomes stable at radius R_c=0.2λ, 0.3λ and 0.5λ for 2, 4 and 8 elements respectively. Thus, these curves can be used to achieve the optimum compactness for practical antennas. It is also noted that when R_c < 0.6λ the system with M_r=4 elements has higher capacity values when including multi-clusters (2, 3 and 5) more than

the M_r=8 system that is modeled assuming one cluster. These results show the impact of multi-cluster modeling on the design of compact antenna arrays with optimum system capacity.

Other multi-clusters scenarios are presented in Fig. 8 to investigate capacity for signals arriving at multi-clusters with different AOA's and different amplitudes. Assuming the signals impinge at a relative mean AoA at Θ_c={90^o} for the single cluster case, Θ_c ={90, ϕ} and with PAS amplitudes equal {a1, a2} for the two cluster case and Θ_c={0+ϕ, 90, 180-ϕ} with PAS amplitudes equal {a1, a2, a3} respectively for three cluster case, ϕ is varied in the range [0°:180°]. The capacities for the three cases are plotted versus ϕ at AS=10 and SNR=15 dB. As can be seen, in general, the capacity increases for 2 and 3 clusters cases compared to 1 cluster case. The capacity of the 2nd clusters case increases as ϕ gets further from 90° (the mean AOA of the 1st cluster). It is noted that the 2 and 3 clusters capacity curves have oscillations across the AOA values (due to the oscillations of the spatial correlation function). Also, envelopes for 2 cluster cases curves increases as the relative amplitude of the PAS of the 2nd cluster (a2) increases from 0.1 to 0.9. It is found that the 3 clusters case with equal PAS amplitudes, is an upper bound of the 1 and 2 clusters cases with highest capacity when mean AOAs at {0, 90, 180}. Capacity of MIMO systems employing UCA at the receiver in Rician fading channels is analyzed with multi-clustered approach and presented in Figs. 9 and 10. Fig. 9 plots complementary cumulative distribution function (c.c.d.f.) of the capacities of 4×4 MIMO cases for different Rician distribution K-factor {0, 10, 1000}. For each K factor value the capacity is computed for 1, 2, 3 and 5 clusters assuming the corresponding mean AOA's are {[90], [45, 90], [45, 90, 135], and [0, 45, 90, 135, 180]} respectively. The simulation parameters are AS=10, SNR = 15 dB and 10,000 channel implementations. As shown, increasing the K factor reduces the capacity of the system. This is because the increase in K emphasizes the deterministic part of the channel in eq. (8) and increases the impact of LOS component existence that is not preferable for MIMO systems. It is also observed that for multi-cluster propagations capacity increases as number of clusters increase especially for K=0 (Rayleigh fading) and low K factor values with the slopes of c.c.d.f. curves increases as K factor

increases. Also, it can be seen that the impact of multi-cluster propagations on capacity is reduced as K factor increases as the difference between c.c.d.f. curves decreases and it becomes overlapped for K=1000 (Gaussian propagation case). Similar observations are obtained from Fig. 10 that present 0.1 outage capacity ($C_{0.1}$) against SNR. As expected, capacities increase linearly with SNR. Highest capacity curve is obtained K=0 and number of clusters =3 and lowest capacity curve is the one for K=1000 with single cluster. The effect of K can be considered as an equivalent loss or gain in the SNR for a given fixed capacity. For example, assume single cluster MIMO system is required to have $C_{0.1}$=15 b/s/Hz with K=1000 then SNR=16 is required. However, the same outage capacity can be achieved for K=10 channel with SNR=28. This means that 14 dB SNR losses get the same MIMO system capacity at different fading channels K=10 and 1000.

IV. CONCLUSION

Simulating realistic correlated MIMO channel that is essential to predict the performance of real MIMO systems was the objective of this paper. Thus, the spatial fading correlation and the channel capacity of a $M_t \times M_r$ MIMO system using multi-clustered statistical clustered channel model are investigated. Results are presented for various hybrid ULA/UCA antenna configurations at different channel assumptions. Uniformly spaced linear and circular arrays are compared showing that UCA outperforms ULA on average for the same aperture size. It is discussed that the system with less number of elements could have a higher capacity values when including multi-clusters than systems with higher number of elements that is modeled assuming one cluster. It is concluded that multi-cluster based approach should be considered when performing capacity investigations as it gives more accurate results than the single cluster case. This could lead to more optimum designs in the search for compact antennas. Results show that the central AOA's of the multi-clusters can have a significant impact on the capacity performance. Also, it is shown that Rician fading reduces the capacity gains in comparison to the fully scattering Rayleigh fading where the K factor effect on the capacity can be considered as SNR loss or gain. Multi-cluster propagations capacity increases as number of clusters increases for low K (Rician) and K=0 (Rayleigh) channels. Finally, the paper

shows the impact of multi-cluster propagations on capacity is reduced as K factor increases.

REFERENCES

[1] A. J. Paulraj, D. Gore, R. U. Nabar and H. Bolcskei, "An overview of MIMO communications–A key to gigabit wireless", *Proceedings of the IEEE,* vol. 92, no. 2, pp. 198-218, Feb. 2004.

[2] L. Schumacher, K. I. Pedersen and P. E. Mogensen, "From antenna spacings to theoretical capacities - guidelines for simulating MIMO systems", *The 13th IEEE International Symposium on Personal, Indoor and Mobile Radio Communications*, vol. 2, pp. 587-592, 2002.

[3] U.A. Waheed and D.V. Kishore, "Uplink spatial fading correlation of MIMO channel", *58th IEEE Vehicular Technology Conference,* VTC 2003, vol. 1., pp. 94-98, 2003.

[4] J. Tsai and B. D. Woerner, "The fading correlation of a circular Antenna Array in Mobile Radio enviroment", *IEEE Global Telecommunications Conference,* vol. 5, pp. 3232-3236, 2001.

[5] L. Xin and N. Zai-ping, "Spatial fading correlation of circular antenna arrays with Laplacian PAS in MIMO channels" *IEEE Antennas and Propagation Society International Symposium*, vol. 4, pp. 3697-3700, 2004.

[6] A. Forenza, D. J. Love, and R. W. Heath, "Simplified Spatial Correlation Models for Clustered MIMO Channels With Different Array Configurations" *IEEE Transactions on Vehicular Technology,* vol. 56, no. 4 part 2, pp: 1924-1934, July 2007.

[7] J. P. Kermoal, L. Schumacher, K. I. Pedersen, P. E. Mogensen, and F. Frederiksen, "A stochastic MIMO radio channel model with experimental validation", *IEEE Journal of Selected Areas in Communications,* vol. 20, no. 6, pp. 1211-1226, Aug. 2002.

[8] P. J. Smith and L. M. Grath, "Exact capacity distribution for dual MIMO systems in Ricean fading", *IEEE Communications Letters*, vol. 8, no. 1, pp. 18-20, Jan. 2004.

Dr. Mohab A. Mangoud received his B.S. and M.S. in Electrical Engineering from the Alexandria University, Egypt in 1993 and 1996, respectively. He received his Ph.D degree from University of Bradford, UK in 2001. Later in 2001, He was Senior RF Engineer for EADS -Astrium (formally Matra Marconi Space Lmt.) Hertfordshire, UK, with a space and commercial communications satellites group. From 2002 till 2007, he was Assistant Professor with Electronics and communications Engineering Department, Arab Academy for Science and Technology (AAST) Alexandria, Egypt. In 2006, Dr. Mangoud was Adjunct Professor with The Bradley Department of Electrical & Computer Engineering, Virginia Polytechnic Institute and State University (Virginia Tech.), Blacksburg, Virginia, USA. He is currently Associate Professor of Wireless Communications, Department of Electrical and Electronics Engineering, University of Bahrain, Bahrain. Dr. Mangoud has been a member of the IEEE since 1998. He was a treasurer of Alexandria/Egypt IEEE Subsection in 2003. His current research interests include: space-time MIMO wireless communication systems, optimization techniques for antenna design applications and numerical electromagnetic methods.